JOURNAL OF THERMOPHYSICS AND HEAT TRANSFER
Vol. 20, No. 2, April–June 2006

Microscale Heat and Mass Transport of Evaporating Thin Film of Binary Mixture

Sang-Kwon Wee*
Samsung Advanced Institute of Technology, Suwon 440-600, Republic of Korea
Kenneth D. Kihm†
University of Tennessee, Knoxville, Tennessee 37996
David M. Pratt‡
Wright–Patterson Air Force Base, Dayton, Ohio 45433
and
Jeffrey S. Allen§
Michigan Technological University, Houghton, Michigan 49931

Analytical and computational studies are presented to examine the effect of binary mixture (pentane/decane) on the microscale heat and mass transport of an evaporating meniscus formed inside a two-dimensional slotted pore. Mass conservation in the liquid film is combined with the momentum equations, energy balance, and normal stress balance and then scaled yielding two constitutive equations: 1) a fourth-order, nonlinear, ordinary differential equation for thin-film profile [Eq. (27)] and 2) a first-order, linear, ordinary differential equation for concentration profile [Eq. (30)]. The numerical results showed that the magnitude of distillation-driven capillary stress due to the composition gradient of a binary mixture can be larger than the thermocapillary stress due to temperature gradient while they are acting in opposite direction. Henceforth, the proof-of-concept has been established in that the binary mixture could facilitate improvement of the evaporating thin-film stability. It was also shown that the resulting stress elongated the length of the evaporating thin-film region without degradation of heat transport effectiveness.

Nomenclature

A	=	dispersion constant, J
C	=	accommodation constant
c_1	=	concentration of pentane in mixture
h	=	thin-film thickness, m
h_{fg}	=	latent heat of vaporization, J/kg
K	=	curvature of liquid–vapor interface, 1/m
k	=	thermal conductivity, W/(m · K)
M	=	molecular weight, kg/kmol
$\dot{m}_{\text{evp}}$	=	evaporative mass flux, kg/(m · s)
P	=	pressure, Pa
P^{sat}	=	saturation pressure, Pa
q	=	heat flux, W/m^2
R	=	universal gas constant, J/(kg · K)
T	=	temperature, K
u	=	velocity component in x direction, m/s
V_l	=	molar volume, m^3/mol
x	=	axial coordinate parallel to substrate, m
y	=	spatial coordinate normal to substrate, m
Γ	=	mass flow rate, kg/s
γ	=	slope of surface tension, N/(m · K)
η	=	nondimensional thickness
θ	=	nondimensional temperature
μ	=	dynamic viscosity, N · s/m^2
ν	=	kinematic viscosity, m^2/s
ξ	=	nondimensional coordinate normal to substrate
Π	=	disjoining pressure
Π_d	=	nondimensional disjoining pressure
ρ	=	density, kg/m^3
σ	=	surface tension, N/m
$6\pi A$	=	Hamaker constant, J

Subscripts

i	=	liquid–vapor interface
id	=	ideal
l	=	liquid
n	=	index of component
v	=	vapor
w	=	wall
0	=	adsorbed film region
1	=	index of pentane
2	=	index of decane

Received 26 January 2005; revision received 10 May 2005; accepted for publication 27 May 2005.

*Researcher, Computational Science and Engineering Center.
†Magnavox Professor, Mechanical, Aerospace and Biomedical Engineering Department; kkihm@utk.edu, Homepage: http://minsfet.utk.edu/.
‡Senior Technical Advisor, Structures Division of Air Vehicles Directorate.
§Assistant Professor, Department of Mechanical Engineering–Engineering Mechanics. Member AIAA.

I. Introduction

THE formation of "tears" in a glass of strong wine (Fig. 1) is a commonly observed example of surface-tension-driven flow resulting from distillation of the more volatile component of a binary liquid. The earliest correct description of this phenomenon was by Thomson[1] in 1855. Preferential evaporation of the more volatile alcohol component ($\sigma = 0.0223$ N/m at 20°C) of the wine near the glass–wine–air interface, referred to as the contact line region, results in a higher concentration of water ($\sigma = 0.0728$ N/m at 20°C) in the liquid film near the contact line as compared to the liquid film near the bulk liquid. The water-rich contact line region has a higher surface tension than the nondistilled liquid film. The surface tension gradient, or capillary phoretic stress, pulls wine up the glass until the weight of the accumulated wine results in a tear falling back toward the bulk liquid.

The tears-of-wine phenomenon provides an insightful analogy for how to ameliorate the unstable operation of phase-change devices.

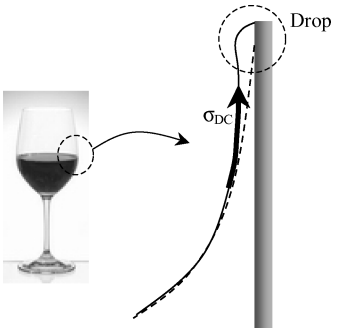

Fig. 1 Tears-of-wine phenomena resulted from distillation-driven capillary stress σ_{DC}.

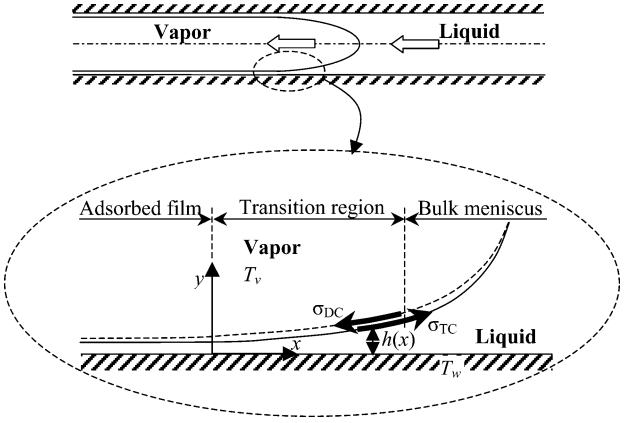

Fig. 2 Schematic of evaporating extended meniscus within two-dimensional slotted pore and distillation-driven capillary stress σ_{DC} and thermocapillary stress σ_{TC}.

During thermally induced evaporation from a meniscus, such as that found in a loop heat pipe, temperature gradients arise from the conjugate phenomena of conductive heat transfer through varying liquid-film thicknesses and nonuniform evaporation due to disjoining pressure affects on the local stress field. The temperature gradient along the thin-film region of a meniscus results in a thermocapillary stress, which drives the surface flow toward the bulk fluid region, thereby reducing the flow of liquid toward the high evaporative flux regions. The thermocapillary stresses are thought to be the primary contributor to the onset of thin-film instability in the contact line region of an evaporating meniscus. It is this thin-film instability that results in unstable operation of phase-change devices, particularly during startup conditions.

If a small amount of a less volatile component is mixed in the more volatile primary working fluid, then perhaps the concentration-induced surface stress can counteract the thermally induced stress and the onset of thin film instability at an evaporating meniscus may be delayed. Figure 2 schematically demonstrates the counteracting surface tensions resulting from the distillation process of a binary mixture and the thermocapillary stress of a pure liquid along the evaporating extended meniscus. The resulting surface tension associated with the binary mixture evaporation, which is called distillation-driven capillary stress, counteracts the thermocapillary stress of pure liquid, and thus, the extended meniscus is elongated due to this counteracting tension. It has been reported experimentally or analytically that an optimum concentration of the binary mixture could lead to the stable thin-film evaporation.[2]

In a series of works by Wayner and his coworkers, the evaporation processes in two-component liquids have been extensively studied experimentally or theoretically. Tung et al.[3] and Wayner et al.[4] conducted experimental studies of an evaporating thin-liquid film formed on an inclined flat substrate immersed in a liquid pool of a mixture. They measured the evaporating extended meniscus profiles of the binary mixture under varying heat flux using a laser interference technique and compared those with the profiles of a pure system. They found that the composition gradient of the mixture in the contact line region has a significant effect on the thin-film profile relative to the pure fluid. They noted that the addition of even a small percentage of a second component (with higher surface tension) significantly influenced the transport processes in the evaporating thin film. The experimental results were analytically examined using a Marangoni flow model by Tung and Wayner.[5] The analysis demonstrated that surface shear resulting from both thermocapillarity and concentration gradient has a significant impact on a multicomponent evaporating system even when the concentration of the second component is small in the bulk fluid.

Recently, Pratt and Kihm[2] experimentally investigated the thermocapillary effects on a heated evaporating meniscus formed with binary mixtures of pentane and decane by measuring the wicking height in capillary pores. They found that an optimum concentration of the binary mixture significantly prolonged instability onset compared to pure liquid. They also demonstrated that there was no significant degrading effect of the binary mixture on heat transport by applying a simple energy balance. Also, the distillation process of a binary mixture for nucleate boiling heat transfer have been studied by Kern and Stephan.[6,7] They developed a theoretical model for the effect of binary mixture evaporation on nucleate boiling heat transfer using a single-bubble model. They described the heat and mass transfer in thin-liquid film and combined the results with macroscopic solution for the liquid and solid domain. Comparison of the heat transfer coefficient of the binary mixture with measurements from experiments showed good agreement. They also demonstrated that the heat transfer in the thin film had a strong influence on overall heat flow.

Parks and Wayner[8] developed a numerical model for a binary mixture evaporating near the contact line region. Combining a constant vapor pressure boundary condition[9] at the liquid–vapor interface with the meniscus profiles from experiments by Tung et al.,[3] they numerically obtained distributions of other physical properties such as concentrations and temperatures in the evaporating meniscus using a thermophysical relationship. They demonstrated that a major contribution to the mass flow rate in the meniscus was surface tension gradients due to gradients in temperature and concentration. They also noted that the surface tension gradient caused by the concentration gradient was more dominant than that by the temperature gradient. However, their analysis needs to be reexamined and improved because they did not calculate the thin-film thickness as a part of the analysis; instead they imposed an experimentally extrapolated polynomial equation for the thin-film profile on their computation.

In the present work, we developed a comprehensive mathematical model to simultaneously and interactively calculate all thermophysical properties as well as the thin-film thickness profiles. The primary goal is to investigate the effect of a binary mixture of a pentane/decane system on heat and mass transport of an evaporating meniscus formed within a two-dimensional slotted pore. The model has been developed in the Cartesian coordinate system and incorporates the thermocapillary effect under nonisothermal condition and the distillation effect of the binary mixture. Based on the distillation model of Parks and Wayner,[9] a differential equation representing the film thickness profile of the evaporating binary mixture has been uniquely developed in nondimensional form. The developed analysis allows comprehensively to predict thin-film profiles, evaporative heat/mass flux distributions along the thin film, interfacial temperature distribution, binary concentration, and resulting surface tension coefficient distributions.

II. Mathematical Formulation

A mathematical model of an evaporating liquid thin film in steady state is considered for a two-dimensional slotted geometry as shown in Fig. 2. The mixture of pentane and decane is assumed to be heated by a uniform heat flux from a solid substrate causing evaporation from the liquid–vapor interface. The wall temperature T_w is held constant, and the vapor phase is assumed to remain in the saturated state at the temperature of T_v. It is postulated that the evaporative flux from the thin film is sustained by constant liquid inflow from the bulk meniscus controlled by gradients in capillary and disjoining pressure. The x–y coordinate origin is set at the junction of the

nonevaporating adsorbed-film region and the evaporating transition film region. The analysis is focused on the transition-film region because previous research has demonstrated that a majority of the heat and mass transport occurs in this region. Therefore, it is in the transition-film region that the interfacial temperature gradient and subsequently the thermocapillary stress peaks.

Because the thermophysical properties are a function of the liquid–vapor interfacial profile, the profile is obtained using the normal stress balance, momentum equation, energy equation, and mass conservation. In the model to describe an evaporation of binary mixture, surface shear due to gradients in concentration and temperature also should be considered.

The transition film region has a very small aspect ratio (h/L) and is a low Reynolds number flow; therefore, the dynamics of liquid flow in the thin-film region can be described by the lubrication theory of fluid mechanics,

$$\mu_l \frac{\partial^2 u}{\partial y^2} = \frac{\mathrm{d}P_l}{\mathrm{d}x} \tag{1}$$

The following boundary conditions are imposed at the solid substrate and the liquid–vapor interface. At $y = 0$,

$$u = 0 \tag{2}$$

At $y = h(x)$,

$$\mu \frac{\mathrm{d}u}{\mathrm{d}y} = \frac{\mathrm{d}\sigma}{\mathrm{d}x} \tag{3}$$

where σ is surface tension. The shear stress resulting from temperature gradients is referred to as thermocapillary stress, and the shear stress resulting from concentration gradients is referred to as distillation-driven capillary stress.[2] The resulting velocity profile in the transition-film region is

$$u(y) = \frac{1}{\mu}\left[\frac{\mathrm{d}P_l}{\mathrm{d}x}\left(\frac{y^2}{2} - hy\right) + \frac{\mathrm{d}\sigma}{\mathrm{d}x}y\right] \tag{4}$$

The mass flow rate over the cross section of height h and unit width is

$$\Gamma = -\frac{h^3}{3\nu_l}\frac{\mathrm{d}P_l}{\mathrm{d}x} + \frac{h^2}{2\nu_l}\frac{\mathrm{d}\sigma}{\mathrm{d}x} \tag{5}$$

where ν_l is the kinematic viscosity of the liquid.

The pressure gradient ($\mathrm{d}P_l/\mathrm{d}x$) results from curvature gradients in the transition-film region. The curvature gradients arise from a balance between capillary forces and disjoining pressure forces described by the well-known augmented Laplace–Young equation,

$$P_v - P_l = \sigma K + \Pi \tag{6}$$

where P_v and P_l are the pressure of the vapor and liquid phases, respectively, Π is the disjoining pressure representing intermolecular interaction force between the liquid and solid, σ is a liquid–vapor interfacial surface tension, and K is a mean curvature of the liquid–vapor interface. The two-dimensional curvature for the slotted pore geometry is

$$K = \frac{\mathrm{d}^2 h}{\mathrm{d}x^2}\left[1 + \left(\frac{\mathrm{d}h}{\mathrm{d}x}\right)^2\right]^{-1.5} \tag{7}$$

where h is the thickness of the film. The curvature in the transition-film region may be linearized. The resulting expression for the curvature is $K \approx \mathrm{d}^2 h/\mathrm{d}x^2$. This linearization of the interface curvature restricts the slope of the liquid–gas interface to be less than 20 deg relative to the solid substrate.[10]

The surface tensions for pure components are related to the local liquid–vapor interfacial temperature using a linear approximation,

$$\sigma_1 = \sigma_{01} - \gamma_1(T_i - T_v) \tag{8}$$

$$\sigma_2 = \sigma_{01} - \gamma_2(T_i - T_v) \tag{9}$$

where the reference surface tension σ_{01} and σ_{02} are for pentane and decane at vapor temperature T_v, respectively, γ_1 and γ_2 are the rate of change of surface tension with temperature, and T_i is the liquid–vapor interfacial temperature. For a binary mixture of low molecular weight alkanes, the effective surface tension can be related to the component surface tensions and concentrations using[11]

$$\sigma = c_1\sigma_1 + (1 - c_1)\sigma_2 \tag{10}$$

where c_1 is the mole fraction of pentane in the mixture. The maximum value of c_1 is one. Combining Eqs. (8–10) yields the expression of effective surface tension for the binary mixture,

$$\sigma = c_1[\sigma_{01} - \gamma_1(T_i - T_v)] + (1 - c_1)[\sigma_{02} - \gamma_2(T_i - T_v)] \tag{11}$$

The surface tension gradient is, therefore, expressed in terms of temperature and concentration gradients,

$$\frac{\mathrm{d}\sigma}{\mathrm{d}x} = [-(\gamma_1 - \gamma_2)c_1 - \gamma_2]\frac{\mathrm{d}T_i}{\mathrm{d}x} + [\sigma_{01} - \sigma_{02} - (\gamma_1 - \gamma_2)(T_i - T_v)]\frac{\mathrm{d}c_1}{\mathrm{d}x} \tag{12}$$

Equation (12) shows that the surface tension gradient is determined by the thermocapillary stress due to temperature gradient and the distillation-driven capillary stress due to the composition gradient.

The disjoining pressure for nonpolar liquids is expressed in the polynomial function of the film thickness in the nonretarded form[12]

$$\Pi = A/h^3 \tag{13}$$

where $6\pi A$ is the Hamaker constant, which is positive for a completely wetting liquid and A is called the dispersion constant or the modified Hamaker constant that accounts for the London–van der Waals forces.

When it is assumed that the vapor pressure does not vary significantly along the transition-film region, the liquid pressure gradient with respect to x is

$$\frac{\mathrm{d}P_l}{\mathrm{d}x} = -\sigma\frac{\mathrm{d}K}{\mathrm{d}x} - K\frac{\partial\sigma}{\partial c_1}\frac{\mathrm{d}c_1}{\mathrm{d}x} - K\frac{\partial\sigma}{\partial T_i}\frac{\mathrm{d}T_i}{\mathrm{d}x} - \frac{\mathrm{d}\Pi}{\mathrm{d}x} \tag{14}$$

As a result, for thin-film evaporation of a binary mixture, the liquid flow is induced by the combined effects of gradients in the curvature, surface tension, concentration, temperature, and disjoining pressure. When the concentration gradient offsets the temperature gradient, the evaporating meniscus may be stabilized.

The concentration gradient can be related to the temperature gradient at the liquid–vapor interface through the use of a constant vapor pressure boundary condition,[9]

$$P_{v_n} = c_n P_{v_n}^{\mathrm{sat}}(T) \tag{15}$$

where $P_{v_n}^{\mathrm{sat}}(T)$ is saturation pressure of component n at temperature T. The vapor pressure of pure components are calculated from the Antoine equation,

$$\ell_n P_{v_n}^{\mathrm{sat}} = A_n + [B_n/(T + C_n)] \tag{16}$$

where the constants for common liquids are given by Reyes and Wayner.[13] The equivalent vapor pressure of the mixture follows Raoult's law, which states that vapor pressure of the mixture is a function of the vapor pressures of the individual components and their mole fraction,

$$P_v = P_{v_1} + P_{v_2} = c_1 P_{v_1}^{\mathrm{sat}}(T_i) + (1 - c_1)P_{v_2}^{\mathrm{sat}}(T_i) \tag{17}$$

where $P_{v_1}^{\mathrm{sat}}$ and $P_{v_2}^{\mathrm{sat}}$ are the saturation vapor pressure of pentane and decane, respectively.

Differentiating Eq. (17) with respect to x and setting the result equal to zero (assuming a constant vapor pressure) yields the following equation:

$$\left(1 - \frac{P_{v_2}^{\mathrm{sat}}}{P_{v_1}^{\mathrm{sat}}}\right)\frac{\mathrm{d}c_1}{\mathrm{d}x} + \left[c_1\frac{\mathrm{d}\,\ell_n P_{v_1}^{\mathrm{sat}}}{\mathrm{d}T} + (1 - c_1)\frac{P_{v_2}^{\mathrm{sat}}}{P_{v_1}^{\mathrm{sat}}}\frac{\mathrm{d}\,\ell_n P_{v_2}^{\mathrm{sat}}}{\mathrm{d}T}\right]\frac{\mathrm{d}T_i}{\mathrm{d}x} = 0 \tag{18}$$

The derivative of concentration may be rearranged as

$$\frac{dc_1}{dx} = \frac{P_{v_1}^{sat}}{P_{v_1}^{sat} - P_{v_2}^{sat}}\left[c_1 \frac{B_1}{(T+C_1)^2} + (1-c_1)\frac{P_{v_2}^{sat}}{P_{v_1}^{sat}}\frac{B_2}{(T+C_2)^2}\right]\frac{dT_i}{dx} \tag{19}$$

The surface tension gradient expressed in Eq. (12) is combined with Eq. (19) yielding the relationship with the temperature gradient alone,

$$\frac{d\sigma}{dx} = \left\{\begin{array}{l} [\sigma_{10} - \sigma_{20} - (\gamma_1 - \gamma_2)(T_i - T_v)]\dfrac{P_{v_1}^{sat}}{P_{v_1}^{sat} - P_{v_2}^{sat}} \\ \quad \times\left[\dfrac{c_1 B_1}{(T+C_1)^2} + \dfrac{P_{v_2}^{sat}}{P_{v_1}^{sat}}\dfrac{(1-c_1)B_2}{(T+C_2)^2}\right] \\ -(\gamma_1 - \gamma_2)c_1 - \gamma_2 \end{array}\right\}\frac{dT_i}{dx} \tag{20}$$

With use of a kinetic theory to relate the net mass flux crossing a liquid–vapor interface to interfacial temperature differential[14] and an extended Clapeyron equation to equate the variation in the equilibrium vapor pressure with temperature and disjoining pressure, the evaporative mass flux escaping from the liquid–vapor interface is given as a function of temperature and pressure jump at the interface,[15]

$$\dot{m}_{evp} = C\left(\frac{M}{2\pi RT}\right)^{\frac{1}{2}}\left[\frac{P_v M h_{fg}}{RT_v T_i}(T_i - T_v) + \frac{V_l P_v}{RT_i}(P_l - P_v)\right] \tag{21}$$

where C is the accommodation coefficient taken to be 2 that is evaluated from the evaporation coefficient,[16,17] M is the liquid molecular weight, V_l is the liquid molar volume at temperature T_i, and h_{fg} is the latent heat of vaporization per unit mass at T_i.

The evaporative heat flux depends on the interfacial temperature. The liquid–vapor interface temperature can be obtained using the steady-state energy equation. The thickness of the liquid film is so small that the conduction heat transfer through the liquid thin film is assumed to be present only in the direction perpendicular to the solid surface. The conduction heat transfer rate would be equal to the evaporation heat flux at the interface. This yields a simplified energy equation resulting in one-dimension conduction equation,

$$\frac{d^2T}{dy^2} = 0 \tag{22}$$

Two boundary conditions are necessary at wall and liquid–vapor interface for obtaining the temperature distribution: At $y = 0$,

$$T = T_w \tag{23}$$

At $y = h$,

$$-k_l \left.\frac{dT}{dy}\right|_{y=h} = \dot{m}_{evp} h_{fg} \tag{24}$$

where k_l is the thermal conductivity of the liquid. These correspond to a specified wall temperature and a balance between conduction and evaporation heat transfer at the liquid–vapor interface, respectively. Solution of energy equation (22) subject to these boundary conditions gives the temperature variation along the interface,

$$T_i(x) = -(\dot{m}_{evp} h_{fg}/k_l)h(x) + T_w \tag{25}$$

With the substitution of the evaporation mass flux given by Eq. (21) into Eq. (25), the interfacial temperature is related with the film thickness, superheat, capillarity, and disjoining pressure.

An evaporative mass flux is related to a mass flow rate in the thin film thorough mass conservation as follows:

$$\frac{d\Gamma}{dx} = -\dot{m}_{evp} \tag{26}$$

The governing equations and boundary conditions are normalized using the following nondimensional variables:

$$\eta = \frac{h}{h_0}, \qquad \xi = \frac{x}{x_0}, \qquad \Pi_d = \frac{\Pi}{\Pi_0} = \frac{1}{\eta^3}$$

$$\dot{m}_{id} = \rho_l u_0, \qquad Ca = \frac{\mu_l u_0}{\sigma_0}, \qquad x_0 = \left(\frac{\sigma_0 h_0}{\Pi_0}\right)^{\frac{1}{2}}$$

$$\theta = \frac{T_i - T_v}{T_w - T_v}, \qquad \kappa = \frac{h_{fg}\dot{m}_{id}}{(k/h_0)}, \qquad \Delta T_0 = T_w - T_v$$

$$\dot{m}_{id} = C\left(\frac{M}{2\pi RT}\right)^{\frac{1}{2}}\left[\frac{P_v M h_{fg}}{RT_v T_i}(T_i - T_v)\right]$$

where h_0 is a thickness of adsorbed film, x_0 is a length of transition film, Π_0 is a disjoining pressure at adsorbed film, $\dot{m}_{id}$ is an ideal mass flux due to temperature differential alone, Ca is capillary number, and κ is the ratio of evaporative interfacial resistance to conductive resistance in the thin film. The specification of scaling variables is based on the work of Hallinan et al.[18] Substituting the mass flow rate [Eq. (5)] and the evaporative mass flux [Eq. (21)] into the relationship of the mass conservation [Eq. (26)] yields a fourth-order, nonlinear, ordinary differential equation for the nondimensional film profile:

$$-\left\{\begin{array}{l} -F_1\eta^3(\eta_{\xi\xi}\theta\, c_1)_\xi - (F_2 - 1)c_1\eta_{\xi\xi\xi}\eta^3 - F_2(\eta_{\xi\xi}\theta)_\xi\eta^3 \\ \quad -(F_3 - 1)\eta_{\xi\xi}\eta^3 c_{1\xi} + F_3\eta_{\xi\xi\xi}\eta^3 - 3\eta^{-1}\eta_\xi \\ \quad + F_4\eta^2[(1 - F_3)c_{1\xi} - F_1(c_1\theta)_\xi - F_2\theta_\xi] \end{array}\right\}_\xi$$

$$= C_1\left\{\theta - [(1 - F_3)c_1 + F_3]\eta_{\xi\xi} + (F_1c_1 + F_2)\theta\eta_{\xi\xi} - \eta^{-3}\right\} \tag{27}$$

where the coefficients are as follows:

$$F_1 = \frac{\gamma_1 - \gamma_2}{\sigma_{01}}\Delta T, \qquad F_2 = \frac{\gamma_2 \Delta T}{\sigma_{01}}, \qquad F_3 = \frac{\sigma_{02}}{\sigma_{01}}$$

$$F_4 = \frac{1.5x_0^2}{h_0^2}, \qquad C_1 = \frac{3\nu_1 x_0^2}{h_0^3 \Pi_0}\dot{m}_{id} \tag{28}$$

Equation (27) for nondimensional film thickness is uniquely formulated in this work. Nondimensional temperature can be expressed in terms of nondimensional thickness and the coefficients from Eq. (25),

$$\theta = \frac{\Delta T_0 + \kappa\left\{[(1 - F_3)c_1 + F_3]\eta\eta_{\xi\xi} + \eta^{-2}\right\}}{\Delta T_0 + \kappa\eta + \kappa\,(F_1c_1 + F_2)\,\eta\eta_{\xi\xi}} \tag{29}$$

and the concentration gradient is also related to the nondimensional temperature in non-dimensional form from Eq. (19),

$$c_{1\xi} = \frac{P_{v_1}^{sat}}{P_{v_1}^{sat} - P_{v_2}^{sat}}\left[c_1\frac{B_1}{(\theta\Delta T + T_v + C_1)^2} + (1 - c_1)\frac{P_{v_2}^{sat}}{P_{v_1}^{sat}}\frac{B_2}{(\theta\Delta T + T_v + C_2)^2}\right]\Delta T\theta_\xi \tag{30}$$

The system of differential equations (27), (29), and (30) can be solved iteratively by Gear's method,[19] which is a higher-order implicit method and designed to solve stiff nonlinear equations with much larger stability limits. The fourth-order differential equation needs four initial conditions at the adsorbed region, $x = 0$. For a completely wetting film, the slope approaches a very small value at the adsorbed film region; thus, the first derivative of the film thickness is zero. The second and third derivatives of the thickness would be zero as well. However, these initial conditions yield the trivial solution of a constant film thickness profile. To avoid these trivial solutions, a small perturbation can be applied to the thickness and

the slope.[20,21] (Note that under small superheat, usually less than 0.01 K, the amount of perturbation is small, and thus, the evaporation mass flux approaches zero at $x = 0$. However, for relatively high superheat, 0.3 K as in our case, a large perturbation is needed to obtain converged solutions. Note that the same perturbations should be used in both calculations of the pure and the mixture cases.) The solution of Eq. (27) is very sensitive to the specification of the initial condition for the second derivative of the thickness especially as the superheat increases. An iterative technique is employed to guess the slope at $x = 0$ such that the solution converges to the appropriate curvature in the bulk meniscus region. Once the liquid-film thickness profile $h(x)$ is obtained from Eq. (27), the other properties are readily determined because they are all functions of $h(x)$, such as temperature [Eq. (29)], pressure gradient [Eq. (14)], and the evaporative mass flux [Eq. (21)].

It is postulated that there be no diffusion associated with the concentration gradient in the y direction (normal to the wall) with the assumption of the uniform concentration across the liquid film at any x location. There would be diffusion in the x direction due to the concentration gradient in the x direction, but this effect is also neglected because the bulk convection may override the diffusion.[8]

III. Results and Discussion

Although the computational effort has been conducted to solve the dimensionless equations (27–30), the results are presented in all dimensional values to provide more intuitive physical meaning for the tested binary mixture and the test conditions. The working fluid is chosen as a mixture of pentane and decane, and the tested geometry is a two-dimensional slotted pore of 2-μm width that can simulate the microscale porous of a heat pipe or a looped heat pipe evaporator. The physical properties of pentane and decane are obtained at 300 K as presented in Table 1, and a saturated vapor condition is assumed. All presented results are under a fixed superheating condition of $\Delta T = 0.3^{\circ}$C. (The range of superheating in this study is constrained to ensure the convergence and stability of the numerical calculations. The wall temperature has a critical effect on the thin-film dynamics. As the wall temperature increases, the superheat increases and it causes a higher temperature gradient along the liquid–vapor interface that makes strong thermocapillary stresses. The thermocapillary stresses lead to an unstable flow in thin-film region under a critical thermal condition and then give rise to a dryout of thin film. The specified 0.3 K is considered as a higher end to provide the calculations to be stable, and for lower superheat values, the calculations converge faster and are more straightforward.) Note that $x = 0$ is set to the point of zero evaporation mass flux as the beginning of the transition region in all of the presented results.

The thin-film profiles of binary mixtures having different concentration ratios of pentane (2% and 10% in volume) are compared to that of pure pentane liquid in Fig. 3, where the evaporating films of binary mixtures are elongated because of the combined action of the thermocapillary stress and the distillation-driven capillary stress (Fig. 2). Such trends are in good agreement with experimental result of Wayner et al.[4] and numerical result of Kern and Stephan.[9] The result demonstrates that the binary mixture could improve the stability of thin-film evaporation by changing the wetting characteristics of the evaporating thin film. [Thermocapillary stresses are known to degrade the wettability of the liquid film by reducing the thin-film length, as seen in many previous works. The degradation of the wettability leads to the unstable evaporation in the thin-film region, and then the liquid film can reach a dryout under critical thermal conditions. Therefore, the elongated film lengths of the binary mixture, in comparison with that of pure liquid under the same thermal conditions (Fig. 3), can be representative of an improvement in the stability of the thin-film evaporation.] Such improvement in the stability was also demonstrated in the experiment using the binary mixture of pentane and decane.[2]

Table 1 Physical properties of pentane and decane at 300 K

Physical properties	Pentane (C_5N_{12})	Decane ($C_{10}N_{12}$)
M, kg/kmol	72.15	142.28
ρ_l, kg/m^3	619	726.4
μ_l, N · s/m^2	2.144×10^{-4}	9.08×10^{-4}
k_l, W/m · K	0.111	0.134
h_{fg}, kJ/kg	361	348.9
σ, N/m	0.04835–1.102×10^{-4}T	0.05079–0.9197×10^{-4}T

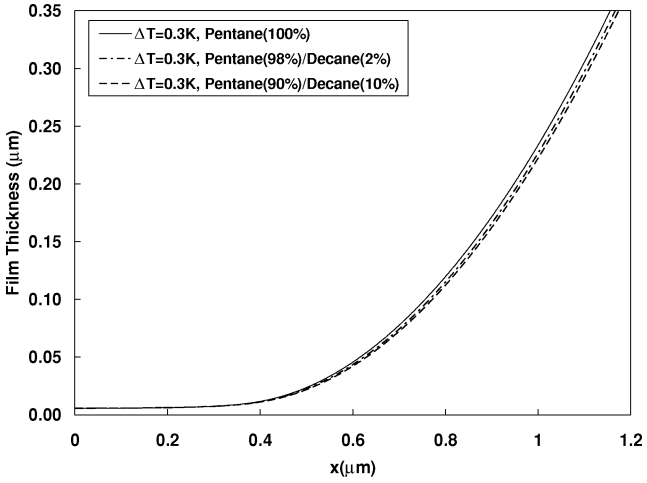

Fig. 3 Comparison of meniscus profiles between pure pentane (100%), mixture of pentane (98%) and decane (2%), and mixture of pentane (90%) and decane (10%) under superheat of 0.3 K.

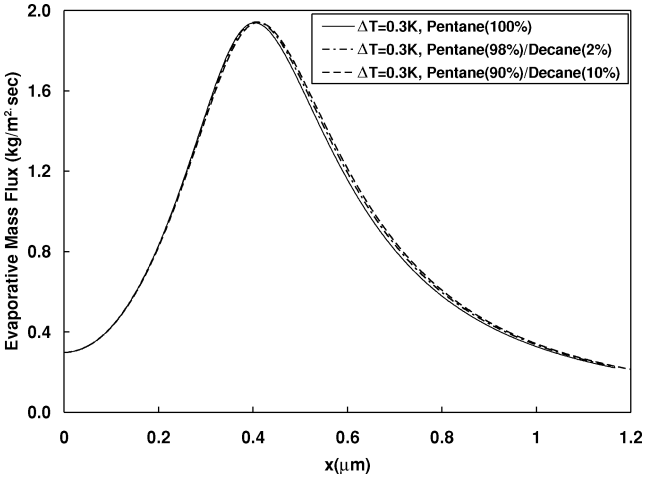

Fig. 4 Comparison of evaporative mass flux between pure pentane (100%), mixture of pentane (98%) and decane (2%), and mixture of pentane (90%) and decane (10%) under superheat of 0.3 K.

Figure 4 shows the comparison of the evaporative mass flux between the pure pentane and the mixtures of pentane and decane at the same superheat of 0.3 K. The evaporative mass flux was calculated from Eq. (21) along the film using the obtained pressure and temperature distribution and thermophysical properties. The distributions of evaporative mass fluxes show a slight increase with an increase in the decane concentration. Thus, adding the small amount of second component does not degrade the heat transport effectiveness of the system.

Figure 5 shows the comparison of interfacial temperature profiles between the mixture and the pure liquid at the superheat of 0.3 K. Note that the gradients in temperature clearly decrease in the transition region of the binary mixture. As explained earlier, the thermocapillary stress is induced due to the temperature gradient, and thus, the lower gradient in the temperature of the binary mixture lead to the smaller thermocapillary stresses, which are counteracted by the distillation-driven concentration gradients. Though the magnitudes of the temperature differentials are minute, note that the tested geometry scale is mere 2-μm wide and such small changes

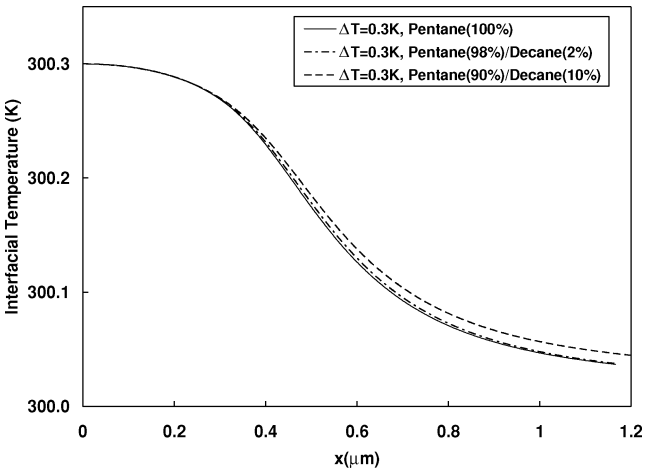

Fig. 5 Comparison of interfacial temperature distribution between pure pentane (100%), mixture of pentane (98%) and decane (2%), and mixture of pentane (90%) and decane (10%) under superheat of 0.3 K.

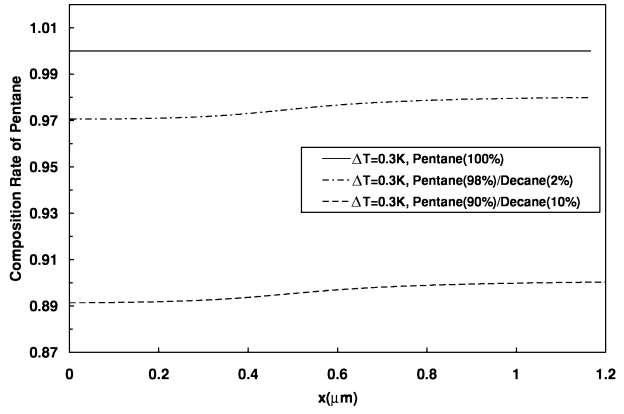

Fig. 6 Comparison of composition rate of pentane between pure pentane (100%), mixture of pentane (98%) and decane (2%), and mixture of pentane (90%) and decane (10%) under superheat of 0.3 K.

in temperature gradients can result in substantial improvement in thermal stability of the transition film.

Figure 6 shows the composition rate of pentane for the three cases of 0, 2, and 10% decane concentrations. For the case of pure pentane, as expected, the rate is constant to be one. In the mixture, the composition rate of pentane varies along the x axis. The pentane concentration at the beginning of transition region ($x = 0$) is reduced by as much as 1% from the bulk mixture concentration for both cases of 2 and 10% pentane. The profiles of the composition rate in the mixture recover to the bulk concentration of 0.98 and 0.9, respectively, as the meniscus region is approached.

Figure 7 shows the comparison of surface tensions between pure pentane and the mixture at the same superheat of 0.3 K. The resulting surface tensions are calculated in Eq. (11) using the interfacial temperature distributions and the composition rates of pentane. For pure liquid, the surface tension increases with increasing x axis, and thus, the resulting surface shear acts toward the bulk meniscus region that causes the transition film region to be shorter. It results from the thermocapillary stress due to temperature gradient along the liquid–vapor interface. On the other hand, for the mixture, the surface tension is reversed, that is, it decreases with increasing x axis, and thus, the resulting surface shear acts toward the thin-film region that causes the transition film region to be longer. It results from the combined effect of the thermocapillary stress and the distillation-driven capillary stress. Thus, the distillation-driven capillary stress can override the thermocapillary stress resulting in a reversed surface tension gradient. Because of such different directions of the resulting surface tensions of the mixture from that of the pure system, the changes in the film length for the pure liquid and the binary mixture occurred as shown in Fig. 3.

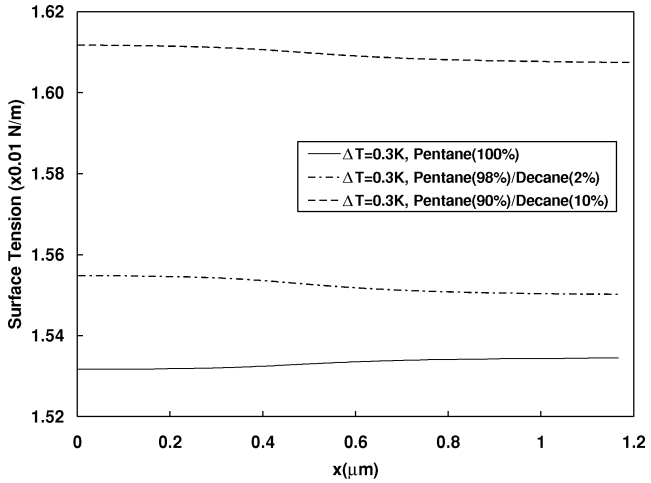

Fig. 7 Comparison of surface tensions between pure pentane (100%), mixture of pentane (98%) and decane (2%), and mixture of pentane (90%) and decane (10%) under superheat of 0.3 K.

For better understanding of the binary mixture evaporation, a scaling analysis[22] can be used to identify the parameters controlling the transition length. First, a characteristic axial velocity u^* is defined using the thin-film mass flux present at the beginning of the thin-film region,

$$u^* = \Gamma_{\rm tr}/\rho_l h_{\rm tr} \tag{31}$$

where the subscript tr refers to conditions at the transition region between the bulk meniscus and the thin film. The transition mass flux can be related to the total heat transfer from the thin film according to

$$\Gamma_{\rm tr} h_{fg} \cong k[(T_w - T_i)/h_{\rm tr}] \cdot L_{\rm tr} \cong k[(T_w - T_v)/h_{\rm tr}] \cdot L_{\rm tr} \tag{32}$$

Here $L_{\rm tr}$ is the length of the thin film. The transition film length can be scaled using the lubrication form of the x-momentum equation. The liquid pressure of Eq. (1) is replaced by the capillary force and disjoining pressure relation of Eq. (6); then consideration of the linear approximation of the derivative of capillary force and disjoining pressure in the transition region, that is, the length $L_{\rm tr}$, and scaling derivatives in u yields

$$u^* \Big/ h_{\rm tr}^2 \cong \bar{K}[(\sigma_0 - \sigma_{\rm tr})/L_{\rm tr}] + [(\Pi_0 - \Pi_{\rm tr})/L_{\rm tr}] \tag{33}$$

where subscript 0 refers to the conditions at the adsorbed region. Equation (33) is rearranged with respect to $L_{\rm tr}$,

$$L_{\rm tr} \cong \{[\bar{K}(\sigma_0 - \sigma_{\rm tr}) + (\Pi_0 - \Pi_{\rm tr})]/u^*\} \cdot h_{\rm tr}^2 \tag{34}$$

Equation (34) shows that the transition-film length increases for the condition of $\sigma_0 > \sigma_{\rm tr}$, which is realized due to the distillation process of the binary mixture, and the trend of the transition-film length was confirmed in Fig. 3. The distribution of the surface tension for the binary mixture was shown in Fig. 7. On the other hand, in the case of the pure liquid evaporation, the temperature gradient along the liquid–vapor interface gives rise to the surface tension gradient of $\sigma_0 < \sigma_{\rm tr}$, and thus, the gradient induces the thermocapillary stresses that reduce the transition-film length.

IV. Summary

A mathematical formulation has been developed to examine the effect of binary mixture evaporation on the fluid flow and heat and mass transfer processes occurring in a two-dimensional slotted pore with depth of 2 μm. The present model is comprehensive in that the thin-film profiles of binary mixtures are directly calculated by overcoming the computational difficulties occurring from the complexity and stiffness of the governing differential equations.

Fundamental findings include the following.

1) The distillation-driven capillary stress of a binary mixture is opposite to the thermocapillary-driven stress, and the former can be compensating the latter resulting a reversed surface tension gradient.

2) The thin-film length of the binary mixture became longer relative to the pure liquid evaporation under the same thermal condition.

3) No noticeable degradation was observed for the heat and mass transport effectiveness of a binary mixture.

Acknowledgment

The authors are grateful to the financial support sponsored by the NASA-Fluid Physics Research Program Grant No. NAG 3-2712 under the technical supervision provided by Mojib Hasan. The presented technical contents are not necessarily the representative views of NASA.

References

[1]Thomson, J., "On Certain Curious Motions Observable at the Surfaces of Wine and Other Alcoholic Liquors," *Philosophical Magazine*, Vol. 10, No. 4, 1855, pp. 330–333.

[2]Pratt, D. M., and Kihm, K. D., "Binary Fluid Mixture and Thermocapillary Effects on the Wetting Characteristics of a Heated Curved Meniscus," *Journal of Heat Transfer*, Vol. 125, No. 5, 2003, pp. 867–874.

[3]Tung, C. Y., Muralidhar, T., and Wayner, P. C., Jr., "Experimental Study of Evaporation in the Contact Line Region of a Mixture of Decane and 2% Tetradecane," *Proceeding of the 7th International Heat Transfer Conference*, Vol. 4, American Society of Mechanical Engineers, Fairfield, NJ, 1982, pp. 101–106.

[4]Wayner, P. C., Jr., Tung, C. Y., Tirumda, M., and Yang, J. H., "Experimental Study of Evaporation in the Contact Line Region of a Thin Film of Hexane," *Journal of Heat Transfer*, Vol. 107, 1985, pp. 182–189.

[5]Tung, C. Y., and Wayner, P. C., Jr., "Effect of Surface Shear on Fluid Flow in an Evaporating Meniscus of a Mixture of Alkanes," *5th International Heat Pipe Conference*, American Society of Mechanical Engineers, Fairfield, NJ, 1984, pp. 201–207.

[6]Kern, J., and Stephan, P., "Theoretical Model for Nucleate Boiling Heat and Mass Transfer of Binary Mixtures," *Journal of Heat Transfer*, Vol. 125, No. 6, 2003, pp. 1106–1115.

[7]Kern, J., and Stephan, P., "Investigation of Decisive Mixture Effects in Nucleate Boiling of Binary Mixtures Using a Theoretical Model," *Journal of Heat Transfer*, Vol. 125, No. 6, 2003, pp. 1116–1122.

[8]Parks, C. J., and Wayner, P. C., Jr., "Surface Shear near the Contact Line of a Binary Evaporating Curved Thin Film," *AIChE Journal*, Vol. 33, No. 1, 1987, pp. 1–10.

[9]Parks, C. J., and Wayner, P. C., Jr., "Fluid Flow in an Evaporating Meniscus of a Binary Mixture in the Contact Line Region: Constant Vapor Pressure Boundary Condition," *AIChE 77th Annual Meeting*, American Inst. of Chemical Engineers, Chicago, 1985, pp. 1–21.

[10]Allen, J. S., "An Analytical Solution for Determination of Small Contact Angles from Sessile Drops of Arbitrary Size," *Journal of Colloid Interface Science*, Vol. 261, No. 2, 2003, pp. 481–489.

[11]Reid, R. C., Prausnitz, J. M., and Sherwood, T. K., *The Properties of Gases and Liquid*, 3rd ed., McGraw–Hill, New York, 1977.

[12]Derjaguin, B. V., and Zorin, Z. M., "Optical Study of the Adsorption and Surface Condensation of Vapours in the Vicinity of Saturation on Smooth Surface," *Proceedings of the Second International Conference on Surface Activity*, edited by J. H. Schulman, Vol. 2, Butterwoods, London, 1957, pp. 145–152.

[13]Reyes, R., and Wayner, P. C., Jr., "Interfacial Models for the Critical Heat Flux Superheat of a Binary Mixture," *32nd National Heat Transfer Conference*, Vol. ASME HTD-342, American Society of Mechanical Engineers, Fairfield, NJ, 1997, pp. 187–194.

[14]Schrage, R. W., *A Theoretical Study of Interphase Mass Transfer*, Columbia Univ. Press, New York, 1953.

[15]Derjaguin, B. V., Nerpin, S. V., and Churaev, N. V., "Effect of Film Transfer upon Evaporation of Liquids from Capillaries," *Bulletin RILEM*, Vol. 29, 1965, pp. 93–98.

[16]DasGupta, S., Schoberg, J. A., and Wayner, P. C., Jr., "Investigation of an Evaporating Extended Meniscus Based on the Augmented Young-Laplace Equation," *Journal of Heat Transfer*, Vol. 115, Feb. 1993, pp. 201–208.

[17]Wayner, P. C., Jr., "Intermolecular Forces in Phase-Change Heat Transfer: 1998 Kern Award Review," *AIChE Journal*, Vol. 45, No. 10, 1999, pp. 2055–2068.

[18]Hallinan, K. P., Chebaro, H. C., Kim, S. J., and Chang, W. S., "Evaporation from an Extended Meniscus for Nonisothermal Interfacial Conditions," *Journal of Thermophysics and Heat Transfer*, Vol. 8, No. 4, 1994, pp. 709–716.

[19]Gear, C. W., *Numerical Initial Value Problems in Ordinary Differential Equations*, Prentice–Hall, Englewood Cliffs, NJ, 1971.

[20]Chebaro, H. C., and Hallinan, K. P., "Boundary Conditions for an Evaporating Thin Film for Isothermal Interfacial Conditions," *Journal of Heat Transfer*, Vol. 115, Aug. 1993, pp. 816–819.

[21]Wayner, P. C., Jr., Kao, Y. K., and LaCroix, L. V., "The Interline Heat-Transfer Coefficient of an Evaporating Wetting Film," *International Journal of Heat and Mass Transfer*, Vol. 19, No. 5, 1976, pp. 487–492.

[22]Wee, S.-K., Kihm, K. D., and Hallinan, K. P., "Effects of the Liquid Polarity and the Wall Slip on the Heat and Mass Transport Characteristics of the Micro-scale Evaporating Transition Film," *International Journal of Heat and Mass Transfer*, Vol. 48, No. 2, 2005, pp. 265–278.